The Multi-Dimensional Crowley Advection Scheme

PIOTR K. SMOLARKIEWICZ

National Center for Atmospheric Research,[1] Boulder, CO 80307

(Manuscript received 24 April 1982, in final form 11 August 1982)

ABSTRACT

The conservation form of the second-order Crowley advection scheme, as some authors have pointed out, may lead to numerical instability for multi-dimensional flows. Replacing the original second-order-accurate approximation of the first spatial partial derivative, with one that includes information about the dimensionality of the field, and also considering the cross-space difference, eliminates this instability without destroying the level of conservation or the accuracy of the original Crowley scheme. The paper also presents some flux correction solutions, the use of which avoids the development of negative values in the solution for positive definite scalars. The paper also discusses the solution of the advection equation in the case of strong deformational flow.

1. Introduction

In the modeling of atmospheric and other geophysical phenomena, it is necessary to calculate the convective transport of some scalar quantities. The Crowley conservative advection scheme is popular, with 74 citations from 1968 to 1979 (Institute for Scientific Information, 1969–80), because of its second-order accuracy in both space and time, and its storage requirement of only one time level.

The original multi-dimensional Crowley scheme was developed in a "time-splitting" form, where one full time step was divided into successive time steps in orthogonal directions. Leith (1965) demonstrated that the second-order numerical approximation of two-dimensional advection is unstable, if the operators for advection in orthogonal directions are combined, and also that the "time-splitting" method produces stable results at least for uniform flow. However, as Petschek and Libersky (1975) have shown, even the time-splitting, two-dimensional Crowley scheme may be weakly unstable in the case of deformational flow. In addition, because of the data transfer, this method is more time-consuming and expensive than a non-time-splitting scheme, especially in the case of three-dimensional modeling.

This paper suggests a method that suppresses instabilities in multi-dimensional advection in cases when simple one-dimensional advection operators are simultaneously used from orthogonal directions. As will be shown later, a new form of the two- or three-dimensional Crowley advection scheme that is stable, at least for uniform flow, can be generated by replacing the original second-order approximation of the first spatial partial derivative (which only considers points on one line), with another approximation that considers points from a plane or a cube. This new form also includes an approximation of cross-space derivative terms.

The generation of negative values in solutions for positive definite functions is another disadvantage of the Crowley scheme which has been reported, e.g., by Soong and Ogura (1973). This difficulty, which is typical for higher-order-approximation advection schemes, led to the use of upstream differencing or other low-order schemes, which produce no dispersive "ripples", but suffer from excessive numerical diffusion. In the last ten years another possible resolution of this problem was developed specifically for application to numerical modeling of plasma fluid problems. The flux-corrected-transport (FCT) method, developed by Boris and Book (1973, 1976) and Book *et al.* (1975), and generalized for the multidimensional case by Zalesak (1979), embodies the best of high- and low-order advection schemes. FCT constructs the net transportive flux point by point (nonlinearly), as the weighted average of a flux computed by a low-order and a flux computed by a high-order scheme. The weighting is done in a manner which insures that the high-order flux is used to the greatest extent possible without introducing ripples. Section 7 of the paper will apply the FCT method to both the Crowley combined scheme and to the scheme proposed here. In Section 8, the proposed scheme will be applied to the case of deformational flow.

[1] The National Center for Atmospheric Research is sponsored by the National Science Foundation.

0027-0644/82/121968-16$08.00

2. Development of a two-dimensional stable Crowley scheme

The equation to be solved is the "color" equation describing the advection of a nondiffusive quantity in a flow field. This equation may be written in any of the following forms (see Crowley, 1968, for notation):

The advective form

$$\frac{\partial \psi}{\partial t} + \mathbf{V}\cdot\nabla\psi = 0; \tag{1}$$

the conservation (flux) form

$$\frac{\partial \psi}{\partial t} + \nabla\cdot(\mathbf{V}\psi) - \psi\nabla\cdot\mathbf{V} = 0; \tag{2}$$

or, in the case of nondivergent flow,

$$\frac{\partial \psi}{\partial t} + \nabla\cdot(\mathbf{V}\psi) = 0. \tag{3}$$

To describe compactly the numerical equations which will be used later, it is convenient to use Shuman-type operators (Shuman, 1962). For an arbitrary dependent variable (ϕ) and an independent variable (η), we have

$$\left.\begin{aligned} \bar{\phi}^{\eta} &= [\phi(\eta + \Delta\eta/2) + \phi(\eta - \Delta\eta/2)]/2 \\ \delta_{\eta}\phi &= [\phi(\eta + \Delta\eta/2) - \phi(\eta - \Delta\eta/2)]/\Delta\eta \\ \tilde{\phi}^{\eta} &= [\phi(\eta + \Delta\eta) + \phi(\eta - \Delta\eta)]/2 \end{aligned}\right\}, \tag{4}$$

where η could be any of x, y, z, t. In all advection forms of the schemes discussed in this paper, it is assumed that the velocity components are defined at the same points as the transported field. In the flux forms of the schemes, the velocity components are defined in an appropriately staggered sense.

The basis of the one-dimensional Crowley scheme for uniform flow (V = const) is the Taylor series expansion of the function $\phi(x_i, t)$, about a point (x_i, t_N), where the temporal partial derivatives in (1) are replaced by the spatial derivatives

$$\psi_i^{N+1} = \psi_i^N - u\Delta t \left.\frac{\partial \psi}{\partial x}\right|_i^N + \frac{u^2\Delta t^2}{2}\left.\frac{\partial^2 \psi}{\partial x^2}\right|_i^N + \mathrm{O}(\Delta t^2) + \mathrm{O}(\alpha\Delta x^3), \tag{5}$$

where the Courant number $\alpha = u\Delta t/\Delta x$ and the term $\mathrm{O}(\Delta t^2)$ occur in cases when $u = u(x, t)$. The second-order finite-difference approximation of the first and second spatial partial derivatives leads to the following scheme:

$$\psi^{N+1} = \psi^N - u\Delta t\delta_x\bar{\psi}^{x} + \frac{u^2\Delta t^2}{2}\delta_{xx}\psi, \tag{6}$$

which for nondivergent flow can be written in the conservation form

$$\psi^{N+1} = \psi^N - \delta_x\left(u\Delta t\bar{\psi}^{x} - \frac{u^2\Delta t^2}{2}\delta_x\psi\right). \tag{7}$$

A natural development of the above scheme for the two-dimensional case should have the form

$$\psi^{N+1} = \psi^N - \delta_x\left(u\Delta t\bar{\psi}^{x} - \frac{u^2\Delta t^2}{2}\delta_x\psi\right) - \delta_y\left(v\Delta t\bar{\psi}^{y} - \frac{v^2\Delta t^2}{2}\delta_y\psi\right). \tag{8}$$

But, as Leith (1965) pointed out, this kind of approximation of (3) is unstable, because the cross term $\partial^2\psi/\partial x\partial y$ is missing from the two-dimensional second-order Taylor series expansion of $\psi(x_i, y_j, t)$ about the point (x_i, y_j, t_N), i.e.,

$$\psi_{ij}^{N+1} = \psi_{ij}^N - u\Delta t\left.\frac{\partial \psi}{\partial x}\right|_{ij}^N - v\Delta t\left.\frac{\partial \psi}{\partial y}\right|_{ij}^N + \frac{u^2\Delta t^2}{2}\left.\frac{\partial^2 \psi}{\partial x^2}\right|_{ij}^N + \frac{v^2\Delta t^2}{2}\left.\frac{\partial^2 \psi}{\partial y^2}\right|_{ij}^N + uv\Delta t^2\left.\frac{\partial^2 \psi}{\partial x\partial y}\right|_{ij}^N + \mathrm{O}(\Delta t^2) + \mathrm{O}(\alpha\Delta x^3; \beta\Delta y^3), \tag{9}$$

where $\beta = v\Delta t/\Delta y$.

Eq. (8) may be written in symbolic operator form

$$\psi_{ij}^{N+1} = (I - A - B)\psi_{ij}^N, \tag{10}$$

where I is the unit matrix, and A and B are matrices such that A and B are proportional to the net fluxes in two orthogonal directions. In the case of uniform flow, phase and amplitude errors, as well as a necessary condition for stability, are given by the eigenvalues of the right-hand side of (10). Following Leith, the eigenvalues of a two-dimensional advection operator are

$$\lambda = 1 - \alpha^2(1 - \cos\theta_x) - \beta^2(1 - \cos\theta_y) - i(\alpha\sin\theta_x + \beta\sin\theta_y), \tag{11}$$

where $\theta_x = k_x\Delta x$, $\theta_y = k_y\Delta y$, k_x and k_y are the components of the wavenumber in the x and y directions. Including the second-order approximation of the cross term $\partial^2\psi/\partial x\partial y$ in the form

$$\left.\frac{\partial^2 \psi}{\partial x\partial y}\right|_{ij}^N = \delta_{xy}\bar{\psi}^{xy} \tag{12}$$

in the scheme (8) changes the eigenvalues of the advection operator as follows:

$$\lambda = 1 - \alpha^2(1 - \cos\theta_x) - \beta^2(1 - \cos\theta_y) - \alpha\beta\sin\theta_x\sin\theta_y - i(\alpha\sin\theta_x + \beta\sin\theta_y). \tag{13}$$

The absolute values of eigenvalues for cases (11) and (13) were found numerically for α, β varying from 0.0 to 1.0 in 0.02 increments and for θ_x, θ_y varying from 0 to π (which is equivalent to the wavelength

on a grid space varying from infinity to $2\Delta x$ or $2\Delta y$) in increments of $\pi/48$.

In both cases of (11) and (13), $\max|\lambda|$ for all θ_x, $\theta_y \in [0, \pi]$ was found, respectively: greater than unity for each permutation of α, β (except α or $\beta = 0$) and less than unity if $(\alpha^2 + \beta^2)^{1/2} \leq 0.5$, for each permutation of α, β. The latter is in agreement with the result obtained by Dukowicz and Ramshaw (1979, formula 15). It was also found that diagonal flow ($\alpha = \beta$) is the case of maximum instability, as Petschek and Libersky (1975) suggested, and that the most unstable waves are those for which $\theta_x = \theta_y$. Thus, including the cross term is still not enough to obtain a stable scheme for $(\alpha^2 + \beta^2)^{1/2} \approx 1$. The tensor viscosity method (Dukowicz and Ramshaw, 1979), which includes the approximation of the cross term in the scheme (8), insures the stability of the scheme, but under a strong restriction on the Courant number. This significantly increases computational cost, especially in the three-dimensional case.

From (6), we can see that the second-order-accurate approximation of the first partial derivative, which is the most active term in the scheme, in a two-dimensional case does not contain any information indicating that the flow is really two-dimensional. To include this information, it is enough to use an approximation of the first spatial partial derivative in the form

$$\left.\frac{\partial\psi}{\partial x}\right|_{ij}^{N} = \delta_x \tilde{\bar{\psi}}^{y}_{x}. \tag{14}$$

Replacing the first spatial partial derivatives in the two-dimensional Taylor series expansion in (9), with an expression similar to (14), and including a second-order approximation of $\partial^2\psi/\partial x\partial y$ in the form (12) (omitting the cross term leads to an unstable scheme), and using an approximation of the second spatial partial derivative as in the Crowley scheme

$$\left.\frac{\partial^2\psi}{\partial x^2}\right|_{ij}^{N} = \delta_{xx}\psi, \tag{15}$$

leads to a second-order finite-difference algorithm for (1) in the form

$$\psi^{N+1} = \psi^N - u\Delta t\delta_x\tilde{\bar{\psi}}^{y}_{x} + \frac{u^2\Delta t^2}{2}\delta_{xx}\psi - \Delta tv\delta_y\tilde{\bar{\psi}}^{x}_{y} + \frac{v^2\Delta t^2}{2}\delta_{yy}\psi + uv\Delta t^2\delta_{xy}\bar{\psi}^{xy}. \tag{16}$$

This scheme may also be written in the flux form

$$\psi^{N+1} = \psi^N - \delta_x\left(\Delta tu\tilde{\bar{\psi}}^{y}_{x} - \frac{\Delta t^2u^2}{2}\delta_x\psi - \frac{\Delta t^2u\bar{v}^{xy}}{2}\delta_y\bar{\psi}^{xy}\right) - \delta_y\left(\Delta tv\tilde{\bar{\psi}}^{x}_{y} - \frac{\Delta t^2v^2}{2}\delta_y\psi - \frac{\Delta t^2v\bar{u}^{xy}}{2}\delta_x\bar{\psi}^{xy}\right). \tag{17}$$

The eigenvalues of the scheme presented, for both the advection and the flux form, are

$$\lambda = 1 - \alpha^2(1 - \cos\theta_x) - \beta^2(1 - \cos\theta_y) - \alpha\beta\sin\theta_x \times \sin\theta_y - i(\beta\sin\theta_y\cos\theta_x + \alpha\sin\theta_x\cos\theta_y). \tag{18}$$

As before, the absolute value of λ was calculated, and the stability condition was obtained in the form

$$|\lambda| < 1 \quad \text{if} \quad (\alpha^2 + \beta^2)^{1/2} \leq 0.95 \quad \text{for all} \quad \theta_x, \theta_y \in [0, \pi]. \tag{19}$$

3. The three-dimensional case

Using the same assumption as before, that the first spatial partial derivative should include information about the dimensionality of the flow, the second-order approximation of $\partial\psi/\partial x$ in three dimensions may be written as

$$\left.\frac{\partial\psi}{\partial x}\right|_{ijk}^{N} = \delta_x\tilde{\bar{\psi}}^{yz}_{x}. \tag{20}$$

A second-order Taylor series expansion of $\psi(x_i, y_j, z_k, t)$ about the point (x_i, y_j, z_k, t_N) has the form

$$\psi_{ijk}^{N+1} = \psi_{ijk}^{N} - u\Delta t\left.\frac{\partial\psi}{\partial x}\right|_{ijk}^{N} - v\Delta t\left.\frac{\partial\psi}{\partial y}\right|_{ijk}^{N} - w\Delta t\left.\frac{\partial\psi}{\partial z}\right|_{ijk}^{N} + \frac{u^2\Delta t^2}{2}\left.\frac{\partial^2\psi}{\partial x^2}\right|_{ijk}^{N} + \frac{v^2\Delta t^2}{2}\left.\frac{\partial^2\psi}{\partial y^2}\right|_{ijk}^{N} + \frac{w^2\Delta t^2}{2}\left.\frac{\partial^2\psi}{\partial z^2}\right|_{ijk}^{N} + \Delta t^2uv\left.\frac{\partial^2\psi}{\partial x\partial y}\right|_{ijk}^{N} + \Delta t^2uw\left.\frac{\partial^2\psi}{\partial x\partial z}\right|_{ijk}^{N} + \Delta t^2wv\left.\frac{\partial^2\psi}{\partial z\partial y}\right|_{ijk}^{N} + O(\Delta t^2) + O(\alpha\Delta x^3; \beta\Delta y^3; \gamma\Delta z^3), \tag{21}$$

where

$$\gamma = w\Delta z/\Delta t.$$

Replacing the respective derivatives in (21) with expressions of the type in (20), (12) and (15), leads to a second-order approximation of the three-dimensional form of (1):

$$\psi^{N+1} = \psi^N - \Delta tu\delta_x\tilde{\bar{\psi}}^{yz}_{x} - \Delta tv\delta_y\tilde{\bar{\psi}}^{xz}_{y} - \Delta tw\delta_z\tilde{\bar{\psi}}^{xy}_{z} + \tfrac{1}{2}\Delta t^2u^2\delta_{xx}\psi + \tfrac{1}{2}\Delta t^2v^2\delta_{yy}\psi + \tfrac{1}{2}\Delta t^2w^2\delta_{zz}\psi + uv\Delta t^2\delta_{xy}\bar{\psi}^{xy} + uw\Delta t^2\delta_{xz}\bar{\psi}^{xz} + vw\Delta t^2\delta_{yz}\bar{\psi}^{yz}. \tag{22}$$

This scheme may also be written in the flux form:

$$\psi^{N+1} = \psi^N - \delta_x\left(u\Delta t\tilde{\bar{\psi}}^{zy}_{x} - \frac{u^2\Delta t^2}{2}\delta_x\psi - \frac{\Delta t^2}{2}u\bar{v}^{xy}\delta_y\bar{\psi}^{xy} - \frac{\Delta t^2}{2}u\bar{w}^{xz}\delta_z\bar{\psi}^{xz}\right)$$
$$- \delta_y\left(v\Delta t\tilde{\bar{\psi}}^{zx}_{y} - \frac{v^2\Delta t^2}{2}\delta_y\psi - \frac{\Delta t^2}{2}v\bar{u}^{xy}\delta_x\bar{\psi}^{xy} - \frac{\Delta t^2}{2}v\bar{w}^{yz}\delta_z\bar{\psi}^{yz}\right)$$
$$- \delta_z\left(w\Delta t\tilde{\bar{\psi}}^{xy}_{z} - \frac{w^2\Delta t^2}{2}\delta_z\psi - \frac{\Delta t^2}{2}w\bar{u}^{xz}\delta_x\bar{\psi}^{xz} - \frac{\Delta t^2}{2}w\bar{v}^{yz}\delta_y\bar{\psi}^{yz}\right). \quad (23)$$

The eigenvalues of the advection operators, for both (23) and (22), in the case of uniform flow have the form

$$\lambda = 1 - \alpha^2(1 - \cos\theta_x) - \beta^2(1 - \cos\theta_y) - \gamma^2(1 - \cos\theta_z) - \alpha\beta\sin\theta_y\sin\theta_x - \alpha\gamma\sin\theta_x\sin\theta_z - \beta\gamma\sin\theta_y\sin\theta_z - i(\alpha\sin\theta_x\cos\theta_y\cos\theta_z + \beta\sin\theta_y\cos\theta_x\cos\theta_z + \gamma\sin\theta_z\cos\theta_x\cos\theta_y), \quad (24)$$

where

$$\theta_z = k_z\Delta z.$$

In the same way as before, the stability condition for wavelengths varying between double the space increment and infinity was found:

$$|\lambda| \leq 1 \quad \text{if} \quad (\alpha^2 + \beta^2 + \gamma^2)^{1/2} \leq 0.92 \quad \text{for all} \quad \theta_x, \theta_y, \theta_z \in [0, \pi]. \quad (25)$$

By comparison, replacing expressions of the type (20) in (22) by the expressions like $\delta_x\bar{\psi}^x$ leads to the three-dimensional form of the tensor viscosity method scheme (Dukowicz and Ramshaw, 1979). It was found that this scheme is stable under the strong restriction $(\alpha^2 + \beta^2 + \gamma^2)^{1/2} \leq 0.34$.

4. Properties of the proposed scheme

Two important properties of any numerical scheme are consistency and stability. It is easy to see that when $\Delta t, \Delta x, \Delta y, \Delta z \to 0$, (23) approaches the form of (3), and (22) approaches the form of (1), which ensures consistency. The results obtained from linear stability analysis for the uniform-flow case in (19) and (25) indicate that the proposed scheme is stable, at least for this kind of flow. Another interesting feature of this scheme is that the lower-dimension scheme is a special case of the higher-dimension one. For example, if $\psi(x, y, z, t) \equiv \psi(x, y, t)$, (23) is the equivalent two-dimensional version of scheme (17), and if $\psi(x, y, z, t) \equiv \psi(x, t)$, (23) is the equivalent one-dimensional conservative Crowley's scheme (7). Conservation of the transported value is ensured by the flux form of the scheme. Multiplying (23) by $\psi^{N+1}_{ijk} + \psi^N_{ijk}$ after omitting the terms proportional to Δt, for nondivergent flow, we can obtain an equation for ψ^2:

$$\delta_t\psi^2 + \delta_x[u(2\bar{\psi}^{x^2} - \bar{\psi}^{x^2})] + \delta_y[v(2\bar{\psi}^{y^2} - \bar{\psi}^{y^2})] + \delta_z[w(2\bar{\psi}^{z^2} - \bar{\psi}^{z^2})] + \Delta x^2\psi[\delta_y(v\delta_{xx}\bar{\psi}^y) + \delta_z(w\delta_{xx}\bar{\psi}^z)] + \Delta y^2\psi[\delta_x(u\delta_{yy}\bar{\psi}^x) + \delta_z(w\delta_{yy}\bar{\psi}^z)] + \Delta z^2\psi[\delta_x(u\delta_{zz}\bar{\psi}^x) + \delta_y(v\delta_{zz}\bar{\psi}^y)] + \frac{\Delta y^2\Delta z^2}{2}\psi\delta_x(u\delta_{yyzz}\bar{\psi}^x) + \frac{\Delta x^2\Delta z^2}{2}\psi\delta_y(v\delta_{xxzz}\bar{\psi}^y) + \frac{\Delta x^2\Delta y^2}{2}\psi\delta_z(w\delta_{xxyy}\bar{\psi}^z) + O(\Delta t) = 0. \quad (26)$$

It follows from this that the proposed scheme for nondivergent flow has no sources of "energy" except those proportional to Δx^2, Δy^2, Δz^2 and Δt. For the simple one-dimensional case, (26) can be written in the form

$$\delta_t\psi^2 + \delta_x[u(2\bar{\psi}^{x^2} - \bar{\psi}^{x^2})] + O(\Delta t) = 0, \quad (27)$$

which means that the one-dimensional Crowley scheme for the case when $\delta_x u = 0$ has a source of "energy" of leading order proportional to Δt.

To discuss other properties of the scheme, such as implicit diffusion and dispersion, it is convenient to analyze the dependence of amplitude and phase error on θ_x and θ_y for the two-dimensional case. In Figs. 1a, b, the isolines of constant absolute value of eigenvalue as a function of θ_x and θ_y are presented, for Courant number $(\alpha^2 + \beta^2)^{1/2} = 0.25$ and $\alpha = \beta \approx 0.18$. For all values of $\theta_x, \theta_y \in [0, \pi] |\lambda| < 1$ for the present scheme, while for the Crowley scheme (Fig. 1b) the area of instability covers the region

$$\theta_x, \theta_y \leq \frac{\pi}{2} \text{ (wavelengths } \lambda_x \geq 4\Delta x, \lambda_y \geq 4\Delta y).$$

The amplitude error $\Delta\lambda = 1 - |\lambda|$ is slightly bigger for the proposed scheme than for Crowley's scheme, and increases for short waves. Fig. 1a shows that some boundary $\theta_x + \theta_y \approx \pi$ exists, which divides all the domain of θ_x, θ_y into two parts in which the behavior of $|\lambda|$ is different. For $\theta_x + \theta_y \leq \pi$ the amplitude error is constant on the lines $\theta_x + \theta_y \approx$ const, which, taking into account that $\alpha - \beta =$ const, means that amplitude error is isotropic, that is, constant on the front of a transported wave. The latter does not occur with the Crowley scheme except for short waves $\lambda_x \leq 3\Delta x$,

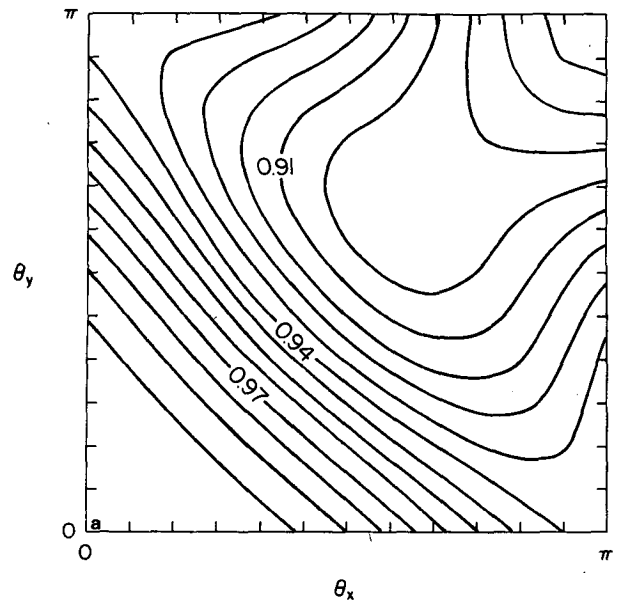

FIG. 1a. Isolines of constant amplitude $|\lambda|$ as a function of phase angles θ_x, θ_y for the proposed scheme. Courant number $(\alpha^2 + \beta^2)^{1/2} = 0.25$, $\alpha = \beta \approx 0.18$, and the contour interval chosen is 0.0075.

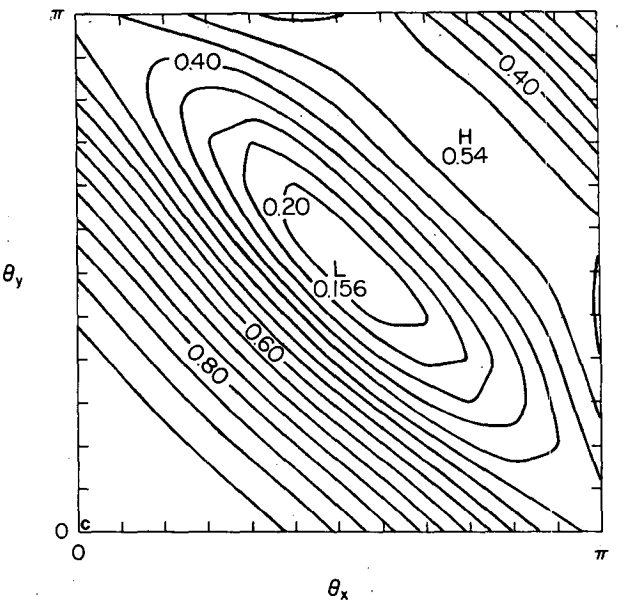

FIG. 1c. As in (a), but for $(\alpha^2 + \beta^2)^{1/2} = 0.75$ and $\alpha = \beta \approx 0.53$, and the contour interval 0.05.

$\lambda_y \leqslant 3\Delta y$. The same conclusion can be found for phase error $\Delta\phi \equiv 1 - \tan^{-1}[\mathrm{Im}(\lambda)/\mathrm{Re}(\lambda)]/(\theta_x\alpha + \theta_y\beta)$ (Fig. 2a, b). For Crowley's scheme (Fig. 2b), the phase error increases for short waves and reaches the value 1, when $\lambda_x = 2\Delta x$ or $\lambda_y = 2\Delta y$, which means that the waves, which have a length of 2Δ at least in one direction, are stationary. For the proposed scheme (Fig. 2a), stationary waves are just those for which $\theta_x + \theta_y \approx \pi$, while the shorter ones ($\theta_x + \theta_y > \pi$) move in a direction opposite to the direction of advection.

Results are shown in Fig. 1c and d for a larger value of the Courant number $(\alpha^2 + \beta^2)^{1/2} = 0.75$ and $\alpha = \beta \approx 0.53$. In the case of the Crowley scheme, the area of instability grows in the direction of the short waves and the amplitude error increases significantly, especially for short waves (Fig. 1d).

For the proposed scheme (Fig. 1c), as for the Crowley scheme, damping increases and reaches a maximum value in the area of stationary waves. Excep-

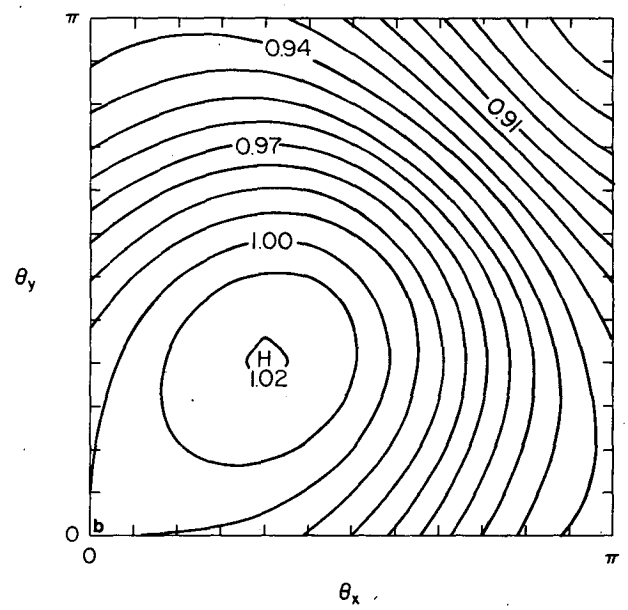

FIG. 1b. As in (a), but for the Crowley combined scheme.

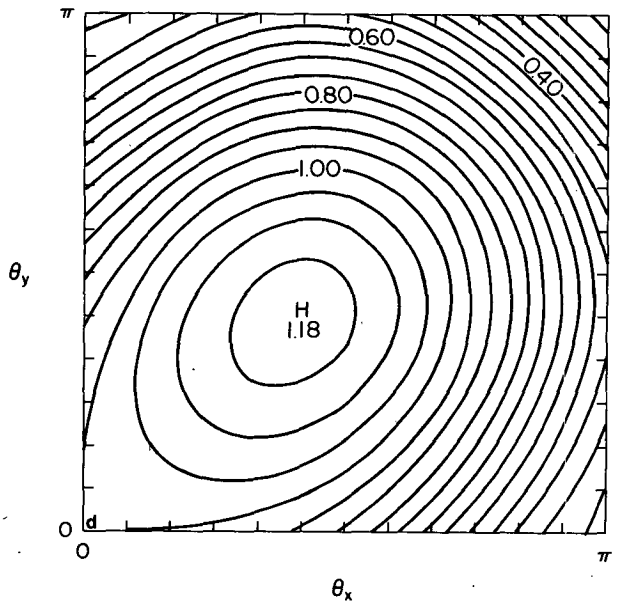

FIG. 1d. As in (c), but for the Crowley combined scheme.

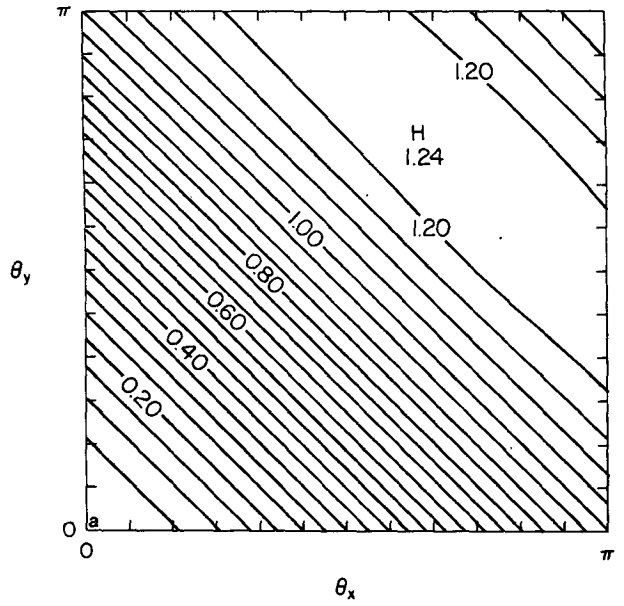

FIG. 2a. Isolines of constant phase error $\Delta\phi$ as a function of phase angles θ_x, θ_y for proposed scheme. Courant number $(\alpha^2 + \beta^2)^{1/2} = 0.25$, $\alpha = \beta \approx 0.18$, and the contour interval chosen is 0.05.

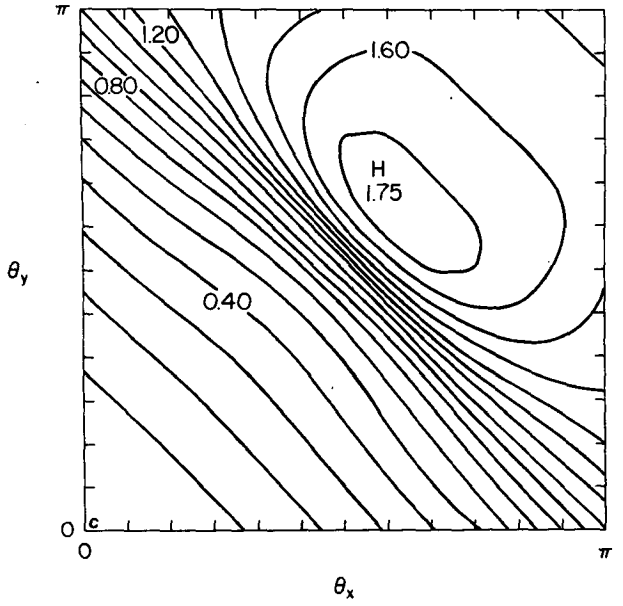

FIG. 2c. As in (a), but for $(\alpha^2 + \beta^2)^{1/2} = 0.75$ and $\alpha = \beta \approx 0.53$, and the contour interval chosen is 0.1.

tionally strong damping can be observed for waves $\lambda_x \approx \lambda_y \approx 4\Delta(\Delta = \Delta x = \Delta y)$. Generally, the short waves are more strongly damped than the long ones. Comparing Figs. 2c and d with 2a and b, one can conclude that, for bigger values of the Courant number, the phase error in the Crowley scheme decreases in the direction of short symmetrical waves, while for the proposed scheme it decreases in the area $(\theta_x + \theta_y < \pi)$ and increases in the remaining part of θ_x, θ_y domain. In the case of nondiagonal flow $(\alpha \neq \beta)$, it is difficult to formulate any general conclusion because of the complicated character of the dependence of the amplitude and phase error on θ_x, θ_y. One can conclude that even in the case of strongly asymmetrical flow, the area of instability for the Crowley scheme decreases only slightly. For both schemes it can be observed that the amplitude and phase error have similar values as in the case of diagonal flow

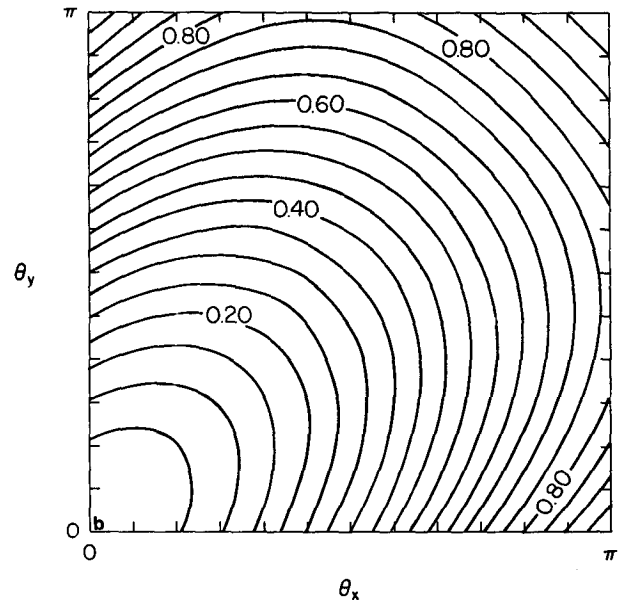

FIG. 2b. As in (a), but for Crowley combined scheme.

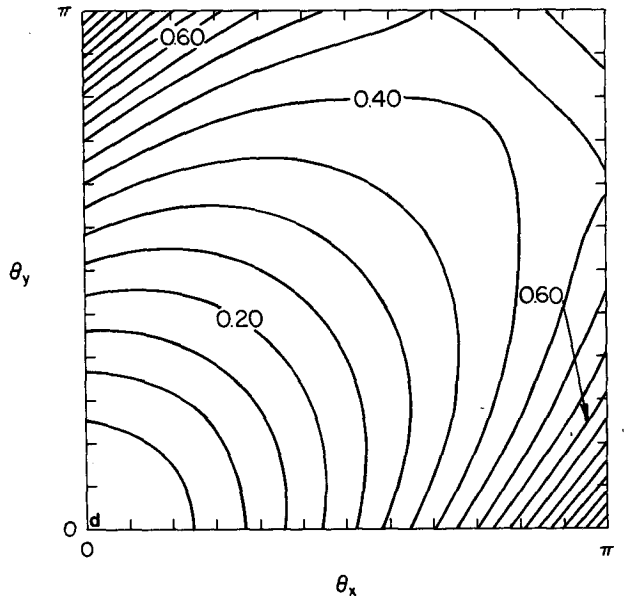

FIG. 2d. As in (c), but for the Crowley combined scheme, the contour interval is 0.05.

(the maximum value is determined by the Courant number rather than the geometry of the flow), but another distribution in the domain of θ_x, θ_y. For the proposed scheme, the area of stationary waves is always associated with strong damping, and waves are never stationary, or move in the direction opposite to convection, if λ_x and λ_y are greater than $4\Delta x$, and $4\Delta y$, respectively. So, the proposed scheme should predict well the transport of waves longer than four grid increments, while the Crowley scheme should better predict the shorter ones.

5. Two-dimensional tests

To show the behavior of the two-dimensional scheme, a solid body rotation test (Crowley, 1968; and Zalesak, 1979) was chosen. The grid space was ($100\Delta x$ by $100\Delta y$), $\Delta x = \Delta y = 1$, the angular velocity $\omega = 0.1$, the maximum Courant number was 0.7, and one full rotation around the point ($50\Delta x$, $50\Delta y$) was equivalent to 628 iterations (i.e., time steps). The initial condition is given in Fig. 3. The maximum and minimum values were FMAX = 3.87 and FMIN = 0, respectively, and the position of the maximum was $Xm = 75\Delta x$, $Ym = 50\Delta y$.

After six full rotations for the proposed scheme (3768 iterations, see Fig. 4), FMAX = 2.59, FMIN = −0.77, $Xm = 72\Delta x$, $Ym = 40\Delta y$, ER1 $\approx 10^{-12}$, and ER2 = 0.06, where ER1 and ER2 are defined as:

$$\left.\begin{aligned} \mathrm{ER1} &= 1 - \left[\int_\Sigma \psi(x, y, t)dxdy \right. \\ &\left. + \int_0^t (\text{outflow})dt\right] \Big/ \int_\Sigma \psi(x, y, 0)dxdy, \\ \mathrm{ER2} &= 1 - \left\{\int_\Sigma \psi^2(x, y, t)dxdy \right. \\ &\left. + \int_0^t [\text{outflow}(\psi^2)]dt\right\} \Big/ \int_\Sigma \psi^2(x, y, 0)dxdy \end{aligned}\right\}, \quad (28)$$

where Σ is the whole domain x, y.

Obviously, after fewer time steps the results are better. For comparison, the results for the two-dimensional Crowley scheme with orthogonal advection operators combined are shown in Fig. 5a for four full rotations. The growing instability can be seen. FMAX = 18.79, FMIN = −18.39, ER1 $\approx 10^{-12}$ and ER2 $\approx -10^3$. To be sure that the instability arising in this case is not forced by the boundary conditions, some tests with dissipative damping of waves close to the boundary were performed. In Figs. 5b–f, examples of the results are presented. The developed instability is shown between the second and the fourth rotation. The time increment between plots is half of one full rotation.

Fig. 6 presents the results for the "upstream" scheme after one rotation: FMAX = 1.30, FMIN = 0, ER1 $\approx 10^{-13}$ and ER2 = 0.68. And Fig. 7 shows the results for the "time-splitting" Crowley scheme after six rotations: FMAX = 3.09, FMIN = −0.59, ER1 $\approx 10^{-12}$, and ER2 = 0.03. In each case the same kind of boundary conditions were used. The second spatial partial derivative in the normal direction was assumed to vanish at the outflow boundary. Vanishing of the first derivative gave practically the same results. The undisturbed initial value of the field was assumed at the inflow boundary.

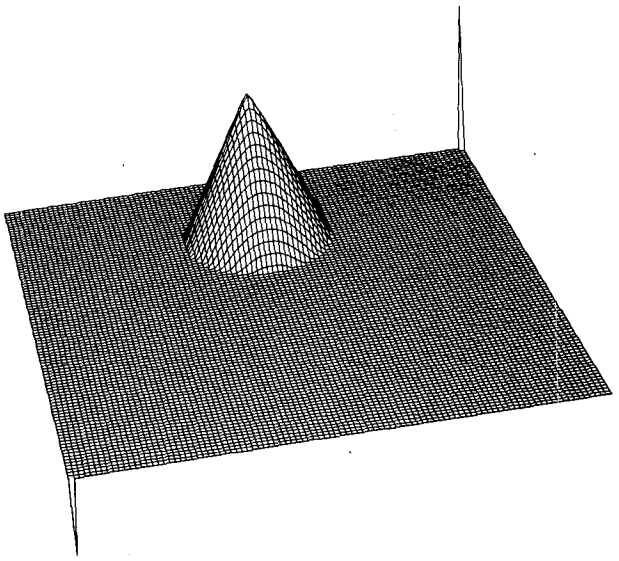

FIG. 3. Initial condition for all two-dimensional tests. Scale values in left-front and right-back corners are −2 and 4, respectively. Maximum value of the initial condition is 3.87.

From a comparison of these results, it can be seen that the best result was obtained in the last case (the time-splitting Crowley scheme gives the same results

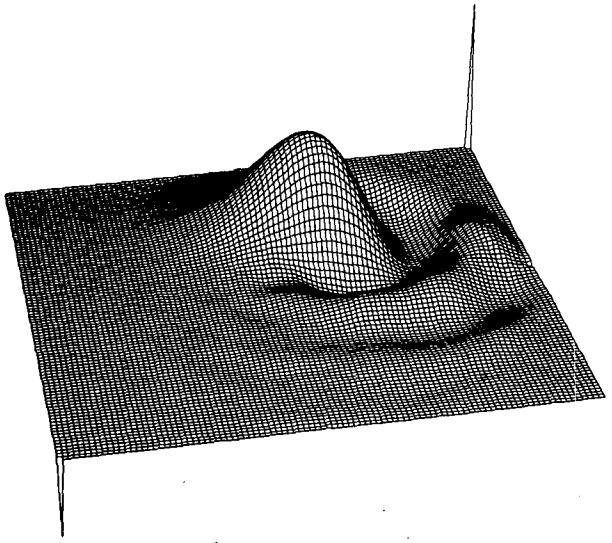

FIG. 4. Solution for the proposed two-dimensional scheme after six full rotations (3768 iterations).

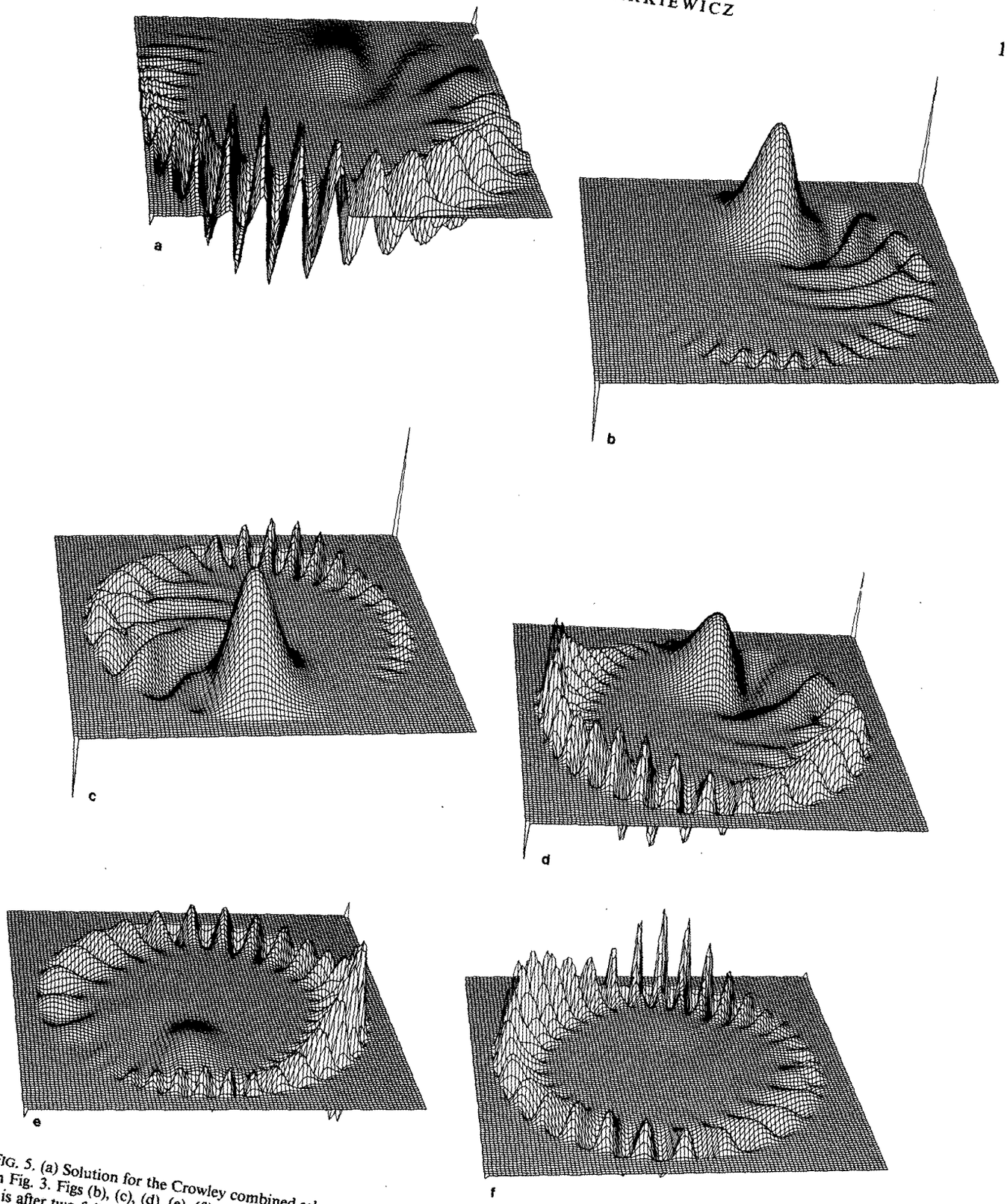

FIG. 5. (a) Solution for the Crowley combined scheme after four full rotations (2512 iterations). Scale values in corners are the same as in Fig. 3. Figs (b), (c), (d), (e), (f) are as in (a), but with additional small dissipative damping of waves close to the boundary. First plot is after two full rotations, time difference between each plot is a half of a rotation.

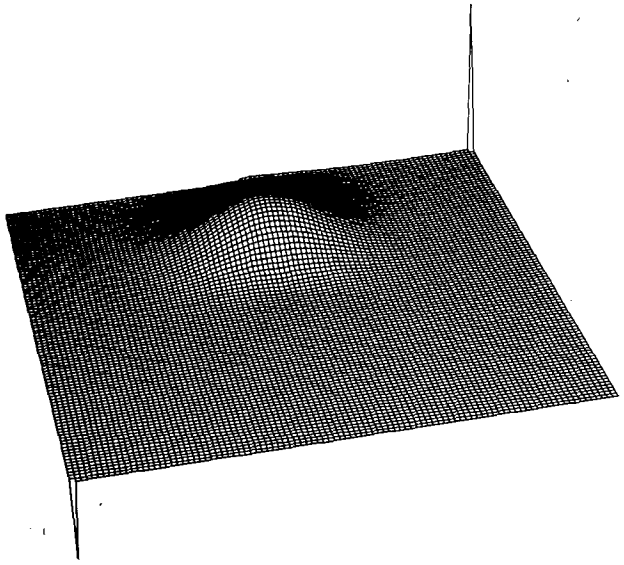

FIG. 6. Solution for "upstream" difference scheme after one rotation (628 iterations).

after six rotations as the proposed version after three rotations) but computing time per iteration is ~33% greater than for the proposed scheme.

6. Three-dimensional tests

As in the previous section, a solid body rotation problem was chosen to present the behavior of the three-dimensional version of the proposed scheme. A sphere with linearly variable density (from 0 on the edge, to a maximum in the center of the sphere) was placed in the center of the grid space ($40\Delta x$ by $40\Delta y$ by $40\Delta z$), (Fig. 8). The sphere is rotating around the diagonal axis of the grid space with angular velocity $\omega = 0.1$. $\Delta x = \Delta y = \Delta z = 2.5$, $\Delta t = 0.25$, and the maximum value of the Courant number is 0.83. Two and a half rotations are equivalent to 628 time steps. Initial conditions are FMAX = 4, FMIN = 0, $Xm = 20\Delta x$, $Ym = 20\Delta y$ and $Zm = 20\Delta z$. After 15 rotations for the proposed scheme (3768 iterations), FMAX = 3.42 and FMIN = −0.06; Xm, Ym and Zm are exactly the same as at the beginning, and ER1 $\approx 10^{-13}$, ER2 = 0.06. In Fig. 9, solution values ≥ 0.5 are presented. As in the previous section, these results were compared with the three-dimensional combined Crowley scheme. Fig. 10 presents the solution after 2.5 rotations (628 iterations): FMAX = 88.11, FMIN = −91.97, ER1 $\simeq 10^{-13}$, and ER2 = −16 by 10^3. Fig. 11 shows the solution for an "upstream" scheme after 2.5 rotations: FMAX = 0.67, FMIN = 0., ER1 $\approx 10^{-13}$, and ER2 = 0.94. Both Figs. 10 and 11 present solutions after a significantly shorter time than Fig. 9, but after five rotations instability fills all the space (Crowley) or the transported initial values vanish (upstream).

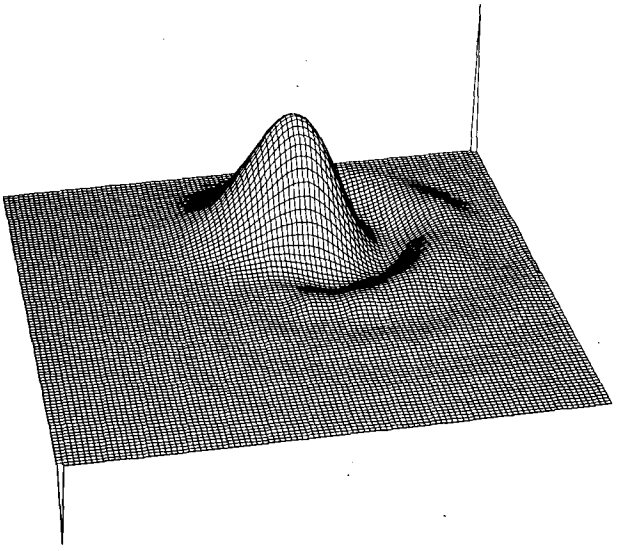

FIG. 7. Solution for Crowley "time-splitting" advection scheme, after six full rotations.

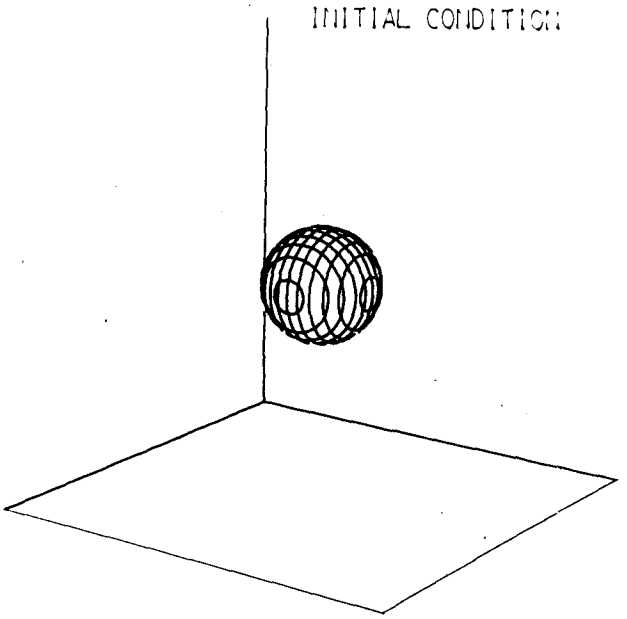

FIG. 8. Initial condition for all three-dimensional tests. All points in which the value of a function is greater than or equal to 0 are plotted. Minimum value 0, maximum value 4.

For all tests the same boundary conditions were used. In the inflow portions of the domain, the boundary condition was formulated as in the previous section. In the outflow portions of the domain, the first spatial partial derivative in a direction normal to a boundary vanishes on the boundary (requiring the second derivative to vanish leads to instability). A three-dimensional version of the "time-splitting" Crowley scheme was not tested because of the excessive computer time required.

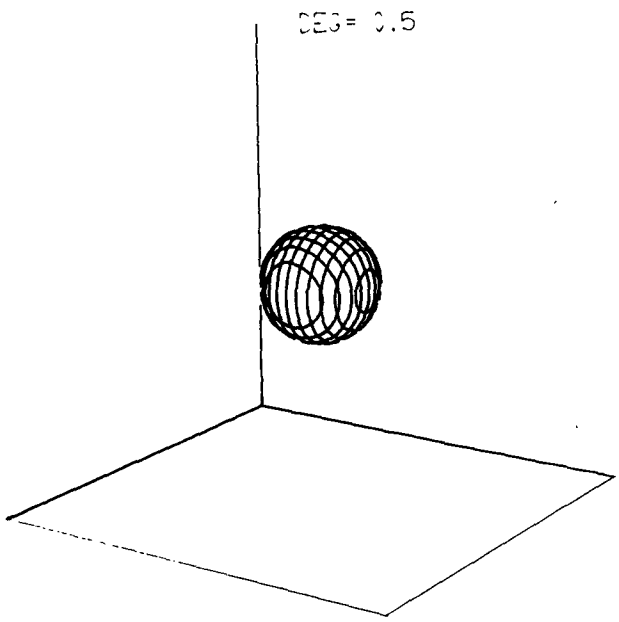

FIG. 9. Solution for three-dimensional version of the proposed scheme after 15 rotations (3768 iterations). The points at which the value of a function is greater than or equal to 0.5 are plotted.

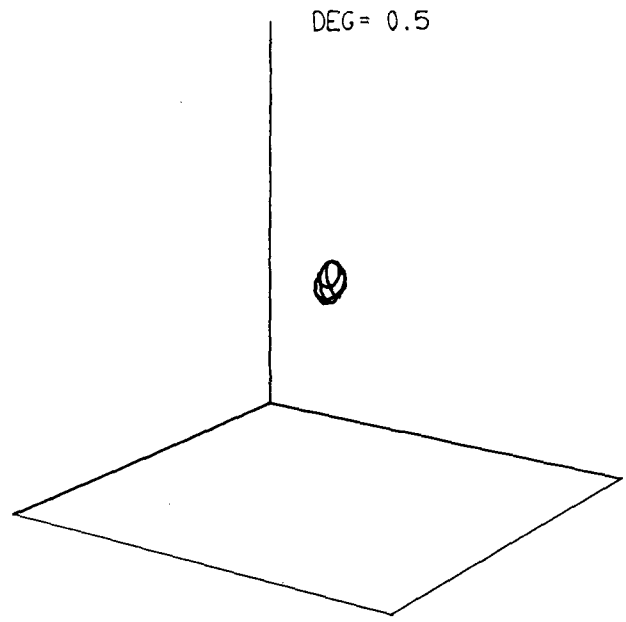

FIG. 11. As in Fig. 9, but for the "upstream" differencing scheme after 2.5 rotations.

7. The flux-correction method

As Soong and Ogura (1973) pointed out, using a Crowley scheme may introduce some difficulties because negative values arise in the solution. This effect can be particularly important in a case when the solution from an advection equation is then used as an input to some nonlinear equations describing micro-

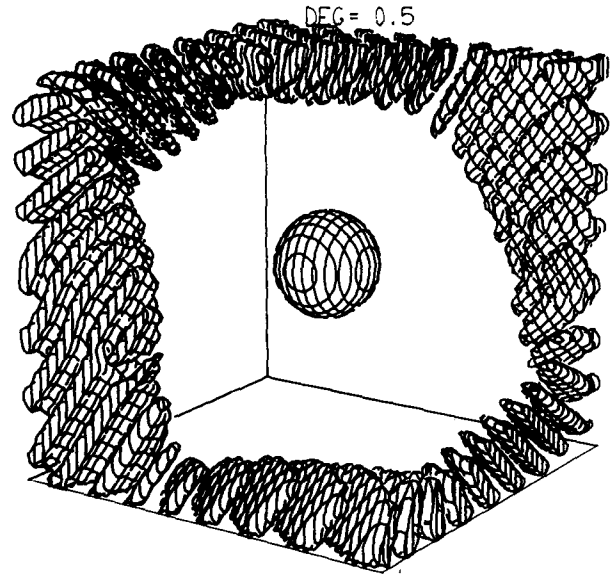

FIG. 10. As in Fig. 9, but for the Crowley combined scheme after 2.5 rotations (628 iterations). Growing instability can be seen around the main solution.

physical phenomena (e.g., the stochastic coalescence equation), which can eventually lead to the instability of the whole system. The rise of negative values of initially positively defined scalar functions during the solution process is typical for all higher-order methods. Care about the positiveness of the solution leads to the use of upstream differencing or other low-order schemes (Soong and Ogura, 1973). To avoid these difficulties without introducing strong implicit diffusion, the use of the flux-corrected-transport (FCT) method, developed by Boris and Book (1973, 1976); Boris *et al.* (1975), and formulated for multidimensional problems by Zalesak (1979), is suggested.

The general form of the FCT algorithm can be written as:

$$\begin{aligned}\psi_{ijk}^{N+1} = \psi_{ijk}^{N} - \{&[\mathrm{CF}\cdot\mathrm{FH} + (1-\mathrm{CF})\cdot\mathrm{FL}]_{(i+1/2)jk} \\ &- [\mathrm{CF}\cdot\mathrm{FH} - (1-\mathrm{CF})\cdot\mathrm{FL}]_{(i-1/2)jk} \\ &+ [\mathrm{CG}\cdot\mathrm{GH} + (1-\mathrm{CG})\cdot\mathrm{GL}]_{i(j+1/2)k} \\ &- [\mathrm{CG}\cdot\mathrm{GH} + (1-\mathrm{CG})\cdot\mathrm{GL}]_{i(j-1/2)k} \\ &+ [\mathrm{CH}\cdot\mathrm{HH} + (1-\mathrm{CH})\cdot\mathrm{HL}]_{ij(k+1/2)} \\ &- [\mathrm{CH}\cdot\mathrm{HH} + (1-\mathrm{CH})\cdot\mathrm{HL}]_{ij(k-1/2)}\}, \quad (29)\end{aligned}$$

where FH, GH and HH are high-order-accuracy fluxes (second order and above), that is, three fluxes in orthogonal directions from any known higher-order-accuracy conservative advection scheme, e.g., Crowley, Lax-Wendroff, or leapfrog.

FL, GL and HL are low-order-accuracy fluxes, e.g., from an "upstream" differencing scheme, a Lax-

Friedrichs, or a high-order scheme with zeroth-order diffusion added. Three matrices of corrective factors $[CF_{(i+1/2)jk}]$, $[CG_{i(j+1/2)k}]$ and $[CH_{ij(k+1/2)}]$, where the value of each factor is less than or equal to 1 and greater than or equal to 0 ($0 < c < 1$), are determined following Zalesak (1979, formulas 6′–13′, and 17′, 18′). [In my experience, the optional use of formulas 14′ (or 14 in the one-dimensional case) gives surprisingly accurate solution for an initial condition which is some kind of step function, but in the case of a smooth initial condition still tends to convert the solution to a step function.] To determine the value of the corrective factor at a certain point, it is necessary to compare the value of the low-order solution with the value of the solution at the previous time in the closest neighborhood of the point being considered. This fact, as well as the construction of corrective factors, ensures that the entire algorithm is stable as long as at least one of the low- or high-order approximation schemes used is stable.

The results of the two-dimensional tests of the FCT method are presented below. In the first case, Crowley's approximation (8) was used as the high-order-approximation fluxes FH and GH; in the second case, the approximation proposed in this paper (17) was used. In both cases, an "upstream" difference approximation was used as the low-order fluxes FL and GL:

$$\left.\begin{aligned} FL_{(i+1/2)j} &= [(u + |u|)_{(i+1/2)j}\psi_{ij} \\ &\quad + (u - |u|)_{(i+1/2)j}\psi_{i+1j}]\frac{\Delta t}{2\Delta x} \\ GL_{i(j+1/2)} &= [(v + |v|)_{i(j+1/2)}\psi_{ij} \\ &\quad + (v - |v|)_{i(j+1/2)}\psi_{ij+1}]\frac{\Delta t}{2\Delta y} \end{aligned}\right\} . \quad (30)$$

For the same initial conditions as in Section 5, the following results were obtained.

Crowley's high-order flux approximation, after six rotations (Figs. 12a, b): FMAX = 3.09, FMIN = -10^{-14}, $Xm = 73\Delta x$, $Ym = 45\Delta y$, ER1 = 10^{-11}, ER2 = 0.28.

The proposed scheme, after six rotations (Figs. 13a, b): FMAX = 2.31, FMIN = 0.0, $Xm = 73\Delta x$, $Ym = 46\Delta y$, ER1 = 10^{-11}, ER2 = 0.35.

As shown above, the unstable combined Crowley scheme becomes stable after use of the FCT method. A comparison between Figs. 12a and b, with 13a and b indicates that the Crowley scheme has slightly smaller damping than the proposed one, but the proposed scheme has better conservation of shape and keeps the symmetry of the initial conditions better. Probably, fourth-order implicit diffusion existing in both schemes is more strongly dependent on smaller velocity in the Crowley scheme than in the proposed scheme (in Fig. 12b it is easy to see that damping is significantly stronger in the direction where velocity vanishes). The FCT method gives the possibility of even better shape conservation (Zalesak, 1979, section V, formulas 19, 20), but significantly increases computing time. Without FCT, the computing times of both schemes are similar. Including the FCT method in its simplest form approximately doubles time consumption.

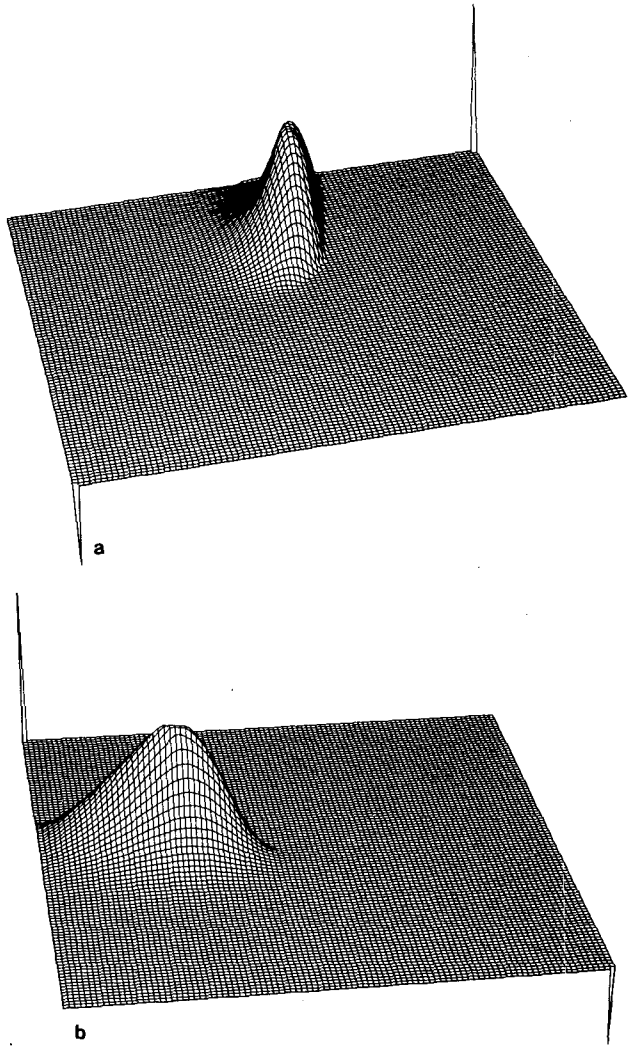

FIG. 12. (a) FCT method for the Crowley combined scheme after six rotations (3768 iterations), (b) seen from another angle.

8. The solution of the advection equation in the case of deformational flow

In the previous sections the simplest possible form of the stable two- and three-dimensional Crowley advection scheme was presented and discussed.

The proposed scheme is not the only one which is possible. Instead of the approximation of the first spatial partial derivative of (14), the following approximation may be used:

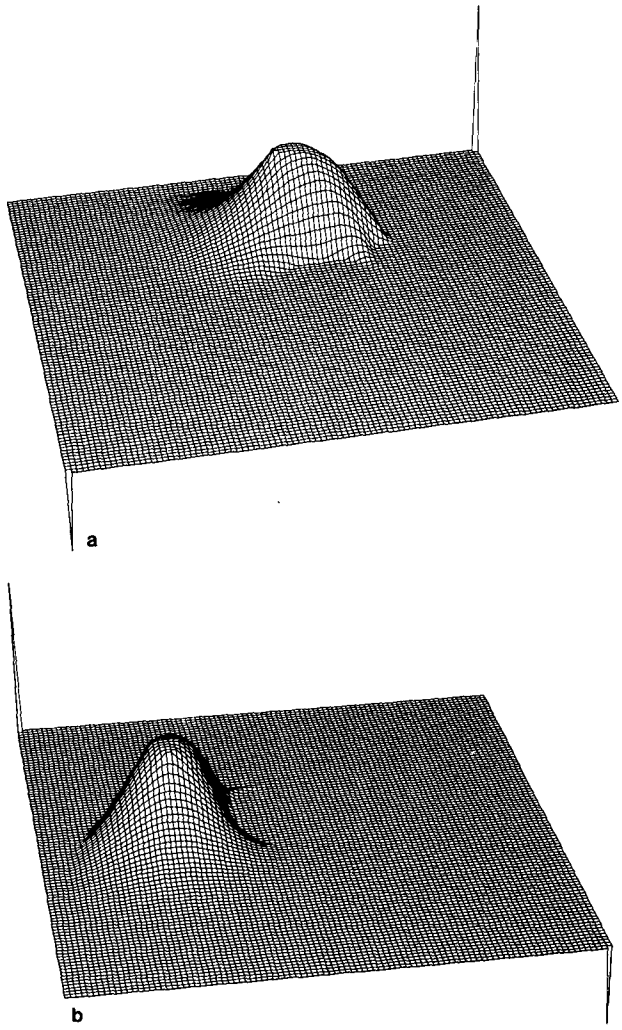

FIG. 13. (a) As in Fig. 12a but for the two-dimensional version of the proposed scheme, (b) seen from another angle.

$$\left.\frac{\partial\psi}{\partial x}\right|_{ij} = \delta_x\bar{\psi}^{xyy}, \tag{31}$$

and instead of the approximation of the second spatial partial derivative (15),

$$\left.\frac{\partial^2\psi}{\partial x^2}\right|_{ij} = \delta_{xx}\bar{\psi}^{yy}, \tag{32}$$

may be used.

Replacing the approximations in (17) of the first and second spatial partial derivatives or only of the first, by expressions of the type in (31) and (32), leads to two new versions of the proposed scheme:

$$\psi^{N+1} = \psi^N - \delta_x\left(\Delta tu\bar{\psi}^{xyy} - \frac{\Delta t^2u^2}{2}\delta_x\bar{\psi}^{yy} - \frac{\Delta t^2u\bar{v}^{xy}}{2}\delta_y\bar{\psi}^{xy}\right) - \delta_y\left(\Delta tv\bar{\psi}^{yxx} - \frac{\Delta t^2v^2}{2}\delta_y\bar{\psi}^{xx} - \frac{\Delta t^2v\bar{u}^{xy}}{2}\delta_x\bar{\psi}^{xy}\right), \tag{33}$$

and

$$\psi^{N+1} = \psi^N - \delta_x\left(\Delta tu\bar{\psi}^{xyy} - \frac{\Delta t^2u^2}{2}\delta_x\psi - \frac{\Delta t^2u\bar{v}^{xy}}{2}\delta_y\bar{\psi}^{xy}\right) - \delta_y\left(\Delta tv\bar{\psi}^{yxx} - \frac{\Delta t^2v^2}{2}\delta_y\psi - \frac{\Delta t^2v\bar{u}^{xy}}{2}\delta_x\bar{\psi}^{xy}\right), \tag{34}$$

[replacing $\delta_{xx}\psi$ in (17) by (32) without replacing $\delta_x\tilde{\bar{\psi}}^{y}_{x}$ leads to an unstable scheme]. The eigenvalues of the advection operator for (33) and (34) are, respectively,

$$\lambda = 1 - \alpha^2(1 - \cos\theta_x)(1 + \cos\theta_y)/2 - \beta^2(1 - \cos\theta_y) \times (1 + \cos\theta_x)/2 - \alpha\beta\sin\theta_x\sin\theta_y - i[\beta\sin\theta_y \times (1 + \cos\theta_x)/2 + \alpha\sin\theta_x(1 + \cos\theta_y)/2], \tag{35}$$

and

$$\lambda = 1 - \alpha^2(1 - \cos\theta_x) - \beta^2(1 - \cos\theta_y) - \alpha\beta\sin\theta_x\sin\theta_y - i[\beta\sin\theta_y(1 + \cos\theta_x)/2 + \alpha\sin\theta_x(1 + \cos\theta_y)/2]. \tag{36}$$

Using the method in Section 2, it was found that in both cases the absolute values of the eigenvalues are less than or an equal to unity if the Courant number $(\alpha^2 + \beta^2)^{1/2}$ is $\leqslant 1$.

These versions of the proposed scheme have properties similar to the first one, except that the behavior of the phase error is rather like that of the original Crowley combined scheme, where all waves move in the direction of advection and the shortest waves ($\lambda_x = 2\Delta x$, $\lambda_y = 2\Delta y$) are stationary. In other words, the above versions have similar properties to the original Crowley combined scheme, except that they are stable even for waves for which the Crowley scheme is unstable. The difference between (33) and (34) is that (34) has significantly stronger damping for short waves (for which $\theta_x + \theta_y \geqslant \pi$).

As long as the scheme is applied to the case of smooth, nondeformational flow, all three presented versions give practically the same results. In Figs. 14a and b, the solution for a solid body rotation test (Section 5) was shown for (33) and (34), respectively. Comparing these results with those presented in Fig. 4, it can be seen that (34) has a slightly smaller damping for long waves than the other versions of the proposed scheme.

Significant differences between different versions of the scheme can be found in the case of deformational flow. In the case of nonuniform flow, it is difficult to prove stability of a scheme which may be dependent on the structure of a velocity field. Therefore, we will discuss some chosen example of strong deformational flow.

On a grid space as in section 5, a stream function was defined as follows:

$$\psi(x, y) = 8 \sin\left[\frac{2\pi}{(L/2)} x\right] \cos\left[\frac{2\pi}{(L/2)} y\right], \quad (37)$$

where $L = 100\Delta x = 100\Delta y(\Delta x = \Delta y = 1)$. Isolines of the streamfunction are shown in Fig. 15a. The velocity field is built up from sets of symmetrical vortices such that their closest neighbors rotate in opposite directions. The maximum value of the Courant number is 0.7, $\Delta t = 0.7$. Deformation of the velocity field is defined as

$$\text{Def} = \frac{\partial u}{\partial x} - \frac{\partial v}{\partial y}. \quad (38)$$

Because of the inequality,

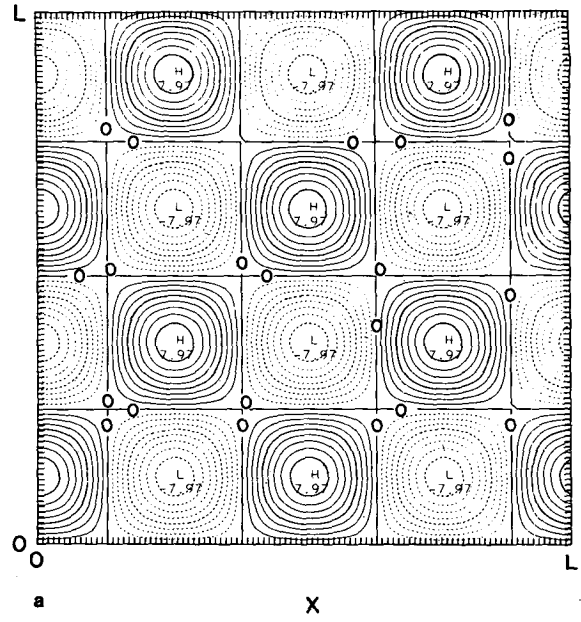

FIG. 15a. Isolines of the stream function for deformational flow tests.

$$\text{Max(Def)} \cdot \Delta t = 1.4 > 1,$$

deformation can be considered to be strong.

As an initial condition (Fig. 15b), the same cone as in Section 5 was placed in the center of the domain. The radius of the base of the cone is slightly greater than the radius of the vortices, so at the initial time, the cone belongs to the area of six vortices, but its main part belongs to the area of the two central ones. It may be expected that after a long enough time, the solution will be divided into two symmetrical pieces

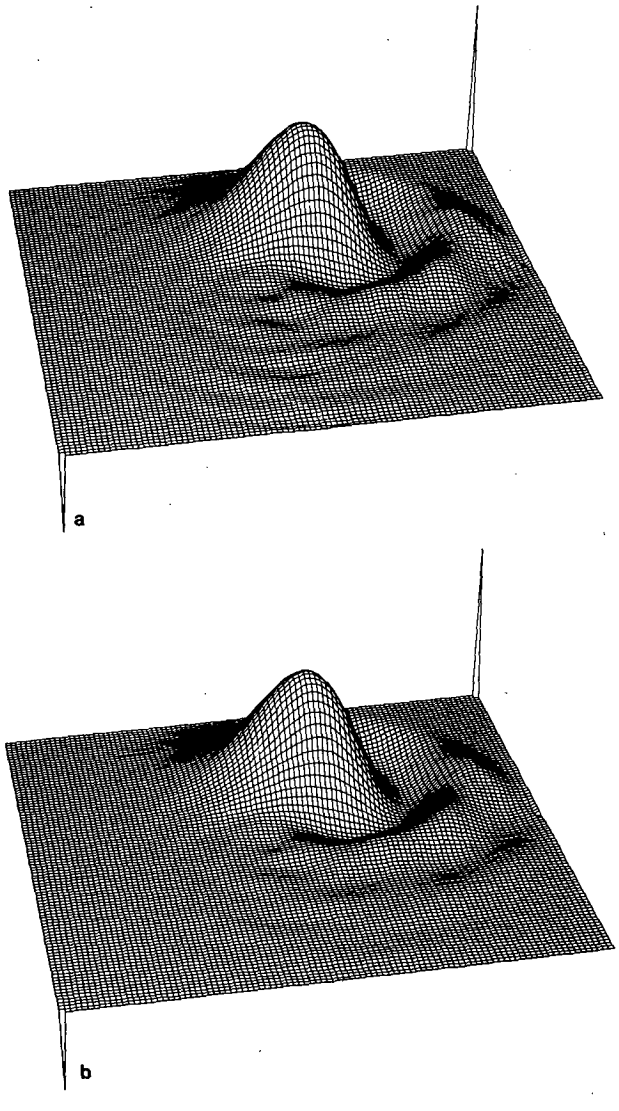

FIG. 14. As in Fig. 4 but for (a) the Eq. (33) version of the scheme, (b) the Eq. (34) version of scheme.

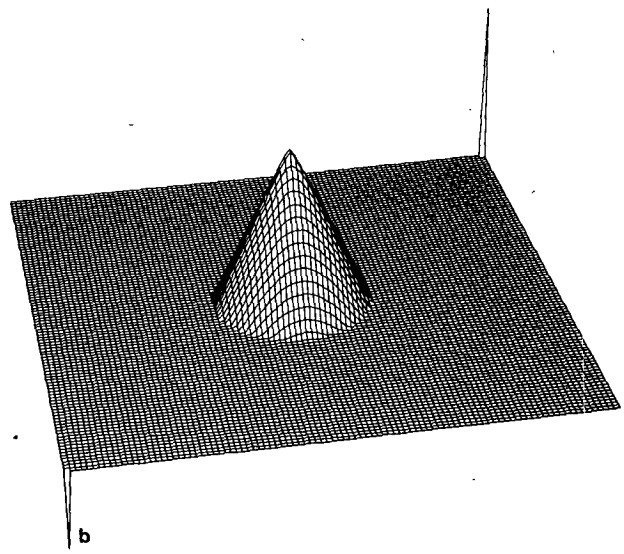

FIG. 15b. As in Fig. 3, but for deformational flow tests.

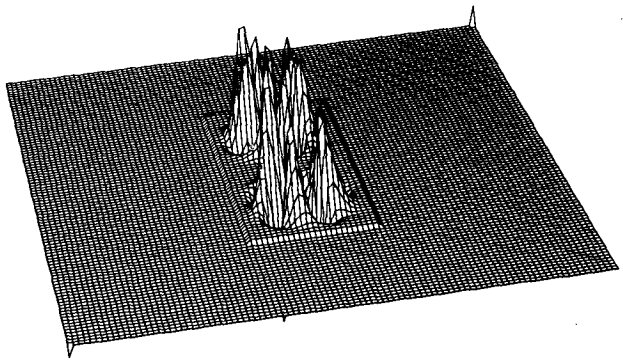

FIG. 16. Solution after 3768 iterations for the Crowley combined scheme in the case of deformational flow.

which will move inside an area of the two central vortices.

In Figs. 16 and 17, the solution after 3768 iterations is shown for the Crowley combined and Crowley "time-splitting" schemes, respectively. In the first case, instability can be observed, as well as the fact that the solution is not divided for the two symmetrical pieces. In the second case, this main feature of the solution can be seen; however, a slowly growing instability (maximum values are twice as big as the initial condition) arises. Fig. 18 also shows the solution after the same number of iterations for the scheme in (34). The solution is stable, but it contains stable stationary short waves with wavelengths $2\Delta x$ and $2\Delta y$. For the version of the proposed scheme in (17), these short waves are strongly unstable, and for (33) they are only weakly unstable. To eliminate the $2\Delta x$, $2\Delta y$ waves, a 17-point spatial filter of Shapiro (1970) was used every ten time steps in the whole domain. This filter results in total elimination of the two-space increment waves with very weak damping of the longer ones. The formula adopted for this filter is given as

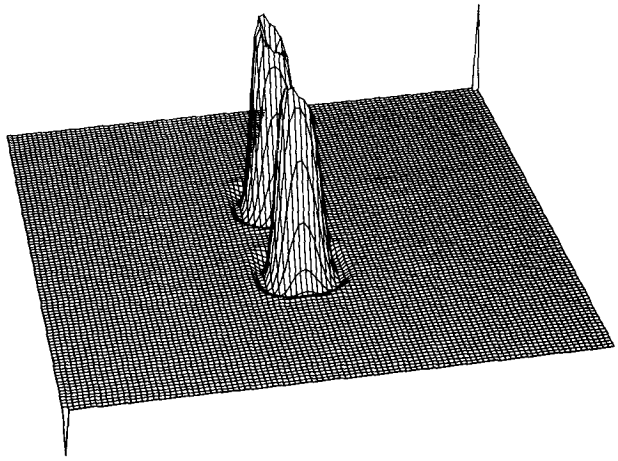

FIG. 17. As in Fig. 16, but for the Crowley "time-splitting" scheme.

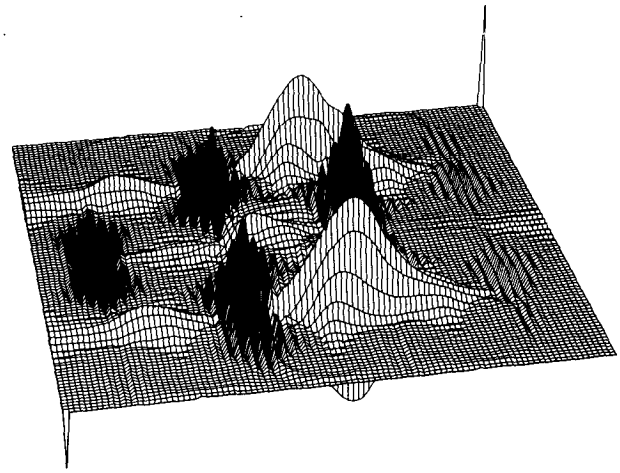

FIG. 18. As in Fig. 16, but for Eq. (34) of the proposed scheme.

$$\psi_i^{\text{filt}} = \psi_i + \frac{(-1)^{n-1}}{4n} \sum_{j=0}^{2n} \frac{(-1)^j (2n)!}{j!(2n-j)!} \psi_{i+n-j}, \quad (39)$$

with $n = 8$ chosen.

In Fig. 19a, a solution after 3768 iterations using version (34) of the proposed scheme is shown with the Shapiro filter applied. The small maximums which can be seen inside both pieces are rotating around the centers of the vortices (because for this case an analytical solution is unknown, the convergence of the solution was shown by doubling the space and time increments). Applying the filter [Eq. (39)] to the versions of (17) and (33) gives similar results (Figs. 19b and c, respectively). In the first case, some small-amplitude $2\Delta x$, $2\Delta y$ waves can be seen. These waves arise so quickly that even a once every ten-time-step filter is not able to eliminate them totally. If the filter is used every third time step, the short waves vanish. In the second case [Eq. (33), Fig. 19c], some residue of the initial condition can be observed in the area of these four vortices that contained some small part of an initial condition at the initial time. This effect is due to the fact that (33) has smaller damping for asymmetrical waves than (17) or (34).

The same filter applied to the original Crowley combined and Crowley "time-splitting" schemes does not change the results shown in Figs. 16 and 17, which is not surprising because the instability arising in both cases is due to the long waves rather than to the short ones. In Figs. 20a and b the results for FCT Crowley and FCT version of (17) of the proposed scheme are presented, respectively. The results are stable in both cases; however, the main features of the solution are lost.

Summarizing the results it can be concluded that (33) and (34) give better results than (17). Three-dimensional equivalents of two-dimensional schemes [Eqs. (33) and (34)] may be obtained in the same way as was presented in Section 3, and they have the re-

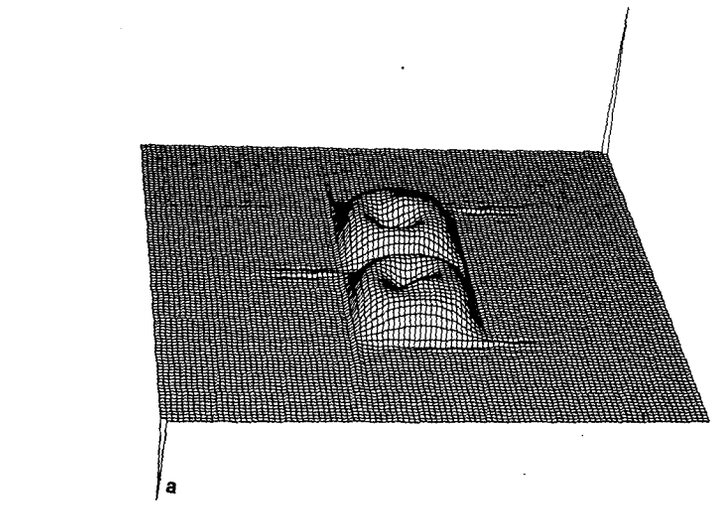

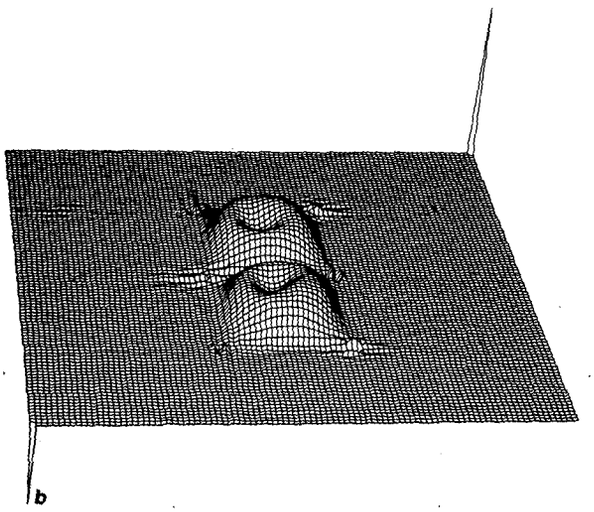

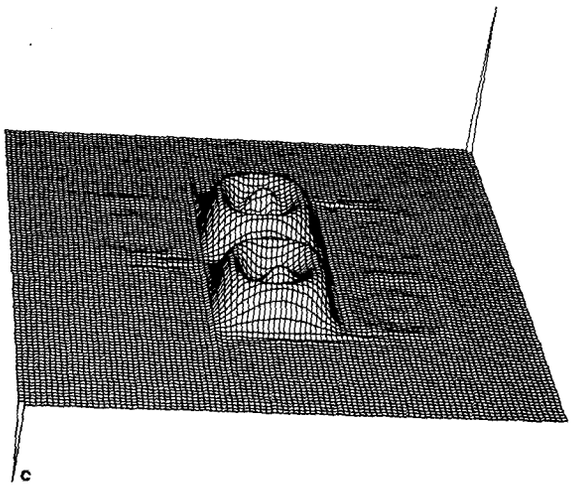

FIG. 19. Solution after 3768 iterations with the Shapiro filter applied to the schemes of (a) Eq. (34), (b) Eq. (17), (c) Eq. (33).

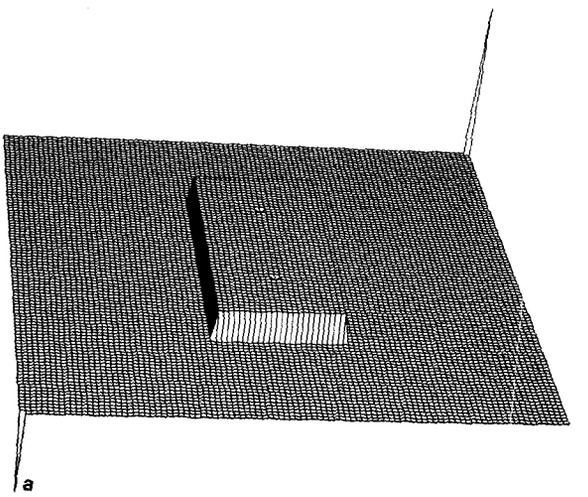

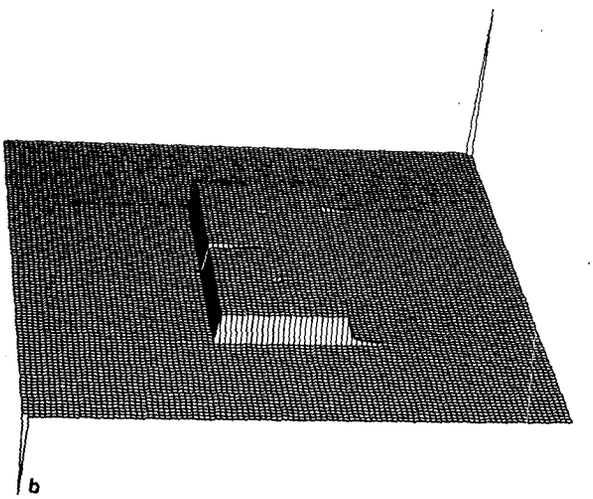

FIG. 20. Solution after 3768 iterations with FCT applied to (a) Crowley combined scheme, (b) scheme of Eq. (17).

spective forms

$$\psi^{N+1} = \psi^N - \delta_x\left(u\Delta t\bar{\psi}^{xyyzz} - \frac{u^2\Delta t^2}{2}\delta_x\bar{\psi}^{yyzz} - \cdots\right) - \delta_y\left(v\Delta t\bar{\psi}^{yxxzz} - \frac{v^2\Delta t^2}{2}\delta_y\bar{\psi}^{xxzz} - \cdots\right) - \delta_z\left(w\Delta t\bar{\psi}^{zxxyy} - \frac{w^2\Delta t^2}{2}\delta_z\bar{\psi}^{xxyy} - \cdots\right), \quad (40)$$

and

$$\psi^{N+1} = \psi^N - \delta_x(u\Delta t\bar{\psi}^{xyyzz} - \cdots) - \delta_y \times (v\Delta t\bar{\psi}^{yxxzz} - \cdots) - \delta_z(w\Delta t\bar{\psi}^{zxxyy} - \cdots), \quad (41)$$

[the terms which are not written explicitly are the

same as in Eq. (23)]. It was found that the above schemes are stable if $(\alpha^2 + \beta^2 + \gamma^2)^{1/2} \leqslant 1$ and $(\alpha^2 + \beta^2 + \gamma^2)^{1/2} \leqslant 0.94$, respectively. In the three-dimensional case, the version of the scheme which has no equivalent in the two-dimensional problem can be found:

$$\psi^{N+1} = \psi^N - \delta_x\left(\cdots - \frac{\Delta t^2}{2} u\bar{v}^{xy}\delta_y\bar{\psi}^{xyzz} - \frac{\Delta t^2}{2} u\bar{w}^{xz}\delta_z\bar{\psi}^{xzyy}\right) - \delta_y\left(\cdots - \frac{\Delta t^2}{2} v\bar{u}^{xy}\delta_x\bar{\psi}^{xyzz} - \frac{\Delta t^2}{2} v\bar{w}^{yz}\delta_z\bar{\psi}^{yzxx}\right) - \delta_z\left(\cdots - \frac{\Delta t^2}{2} w\bar{u}^{xz}\delta_x\bar{\psi}^{xzyy} - \frac{\Delta t^2}{2} w\bar{v}^{yz}\delta_y\bar{\psi}^{yzxx}\right), \tag{42}$$

[the terms which are not written explicitly are the same as in Eq. (40)]. The above scheme is stable if $(\alpha^2 + \beta^2 + \gamma^2)^{1/2} \leqslant 1$. In the three-dimensional case, as well as in the two-dimensional one, there exist other possibilities for generating new versions of the scheme, particularly in applications to the atmospheric problems in which the vertical direction is distinctive. This introduces the possibility of constructing asymmetrical schemes with different methods of averaging of the derivative operators in the vertical direction than in the horizontal.

9. Conclusions

1) Replacing the original second-order-accurate approximation of the first spatial partial derivative (which considers points lying on the same line) with one that includes information on field dimensionality (which considers points from a plane or cube, and the cross-space derivatives) leads to a new form of the combined Crowley advection scheme which is stable at least for uniform flow.

2) Use of the FCT method stabilizes the original Crowley combined scheme and gives non-negative solutions. A comparison between the flux-corrected combined Crowley scheme and the flux-corrected scheme proposed in this paper shows that our proposed scheme has slightly stronger implicit diffusion that is less dependent on velocity, and finally leads to a better prediction of the shape of the solution.

3) The proposed scheme may have some different versions, depending on the applied method of averaging of the first and second spatial partial derivative operators. All presented versions gave similar solutions in the case of smooth non-deformational flow, because they have similar properties for long transported waves. In the case of deformational flow, the different versions of the proposed scheme may give different solutions (from strong instability through weak instability to neutral stability for two-space-increment long waves). Filtering the shortest $2\Delta x$, $2\Delta y$ waves again leads to stable similar solutions for different versions of the scheme.

Acknowledgments. The author is extremely grateful to Dr. Terry L. Clark of NCAR for his advice and support in this project as well as for his helpful discussion and criticism of the manuscript. The author also wishes to thank Dr. William D. Hall and James Drake of NCAR for their helpful discussion; Mrs. Marie Boyko for her help correcting the English language in the paper and Mrs. Sharon A. Blackmon and Mrs. Susan J. Thomas for their typing of the manuscript. I wish to acknowledge the support received from the Advanced Study Program of NCAR while doing this research. I am also especially grateful to Dr. Rainer Bleck of the University of Miami for his inspiration of my interests in the advection problem.

REFERENCES

Book, D. L., J. P. Boris and K. Hain, 1975: Flux-corrected transport II: Generalizations of the method. *J. Comput. Phys.*, **18,** 248–283.

Boris, J. P., and D. L. Book, 1973: Flux-corrected transport I: SHASTA, a fluid transport algorithm that works. *J. Comput. Phys.*, **11,** 38–69.

——, and ——, 1976: Flux-corrected transport III: Minimal-error FCT algorithms. *J. Comput. Phys.*, **20,** 397–431.

Crowley, W. P., 1968: Numerical advection experiments. *Mon. Wea. Rev.*, **96,** 1–11.

Dukowicz, J. K., and J. D. Ramshaw, 1979: Tensor viscosity method for convection in numerical fluid dynamics. *J. Comput. Phys.*, **32,** 71–79.

Institute for Scientific Information, 1969–1980: *Science Citation Index.* 1968–1979 Annuals.

Leith, C. E., 1965: Numerical simulation of the earth's atmosphere. Applications in Hydrodynamics, Vol. 4, *Methods in Computational Physics,* Academic Press, 1–28.

Petschek, A. G., and L. D. Libersky, 1975: Stability, accuracy, and improvement of Crowley advection schemes. *Mon. Wea. Rev.*, **103,** 1104–1109.

Shapiro, R., 1970: Smoothing, filtering, and boundary effects. *Rev. Geophys. Space Phys.*, **8,** 359–387.

Shuman, F. G., 1962: Numerical experiments with the primitive equations. *Proc. 1st Symp. on Numerical Weather Prediction,* Tokyo, Meteor. Soc. Japan, 85–107.

Soong, S. T., and Y. Ogura, 1973: A comparison between axisimmetric and slab symmetric cumulus models. *J. Atmos. Sci.*, **30,** 879–893.

Zalesak, S. T., 1979: Fully multi-dimensional flux-corrected transport algorithms for fluids. *J. Comput. Phys.*, **31,** 335–362.